ACS OMEGA

http://pubs.acs.org/journal/acsodf

Article

Phenothiazine Dyes Induce NADH Photooxidation through Electron Transfer: Kinetics and the Effect of Copper Ions

Kazutaka Hirakawa* and Mizuho Mori

Cite This: *ACS Omega* 2021, 6, 8630−8636

Read Online

ACCESS | Metrics & More | Article Recommendations | Supporting Information

ABSTRACT: Phenothiazine dyes, methylene blue, new methylene blue, azure A, and azure B, photosensitized the oxidation of nicotinamide adenine dinucleotide (NADH), an important coenzyme in the living cells, through electron transfer. The reduced forms of these phenothiazine dyes, which were produced through electron extraction from NADH, underwent reoxidation to the original cationic forms, leading to the construction of a photoredox cycle. This reoxidation process was the rate-determining step in the photoredox cycle. The electron extraction from NADH using phenothiazine dyes can trigger the chain reaction of the NADH oxidation. Copper ions enhanced the photoredox cycle through reoxidation of the reduced forms of phenothiazine dyes. New methylene blue demonstrated the highest photooxidative activity in this experiment due to the fast reoxidation process. Electron-transfer-mediated oxidation and the role of endogenous metal ions may be important elements in the photosterilization mechanism.

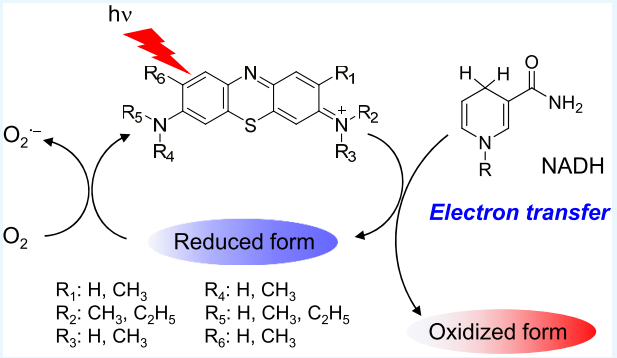

INTRODUCTION

Phenothiazine dyes, such as methylene blue (MB; Figure 1), have been applied as agents for antimicrobial photodynamic therapy (aPDT), which is one of the most important medicinal applications of dyes.[1−5] Specifically, aPDT is an advantageous method to sterilize multidrug-resistant bacteria.[6,7] MB and its derivatives (Figure 1) can absorb long-wavelength visible light (>650 nm).[3,8] Because long-wavelength visible light can penetrate deeply into biomaterials, including human tissue,[9,10] it is important for photobiological and photomedicinal effects. For example, treatments for periodontal disease,[11,12] dental caries,[13,14] and bone infection[15] are important applications of aPDT using phenothiazine dyes with a red light. Furthermore, viral inactivation photosensitized by phenothiazine dyes has been studied.[16,17] These phenothiazine dyes can photosensitize singlet oxygen ($^1O_2$) production with a relatively large quantum yield (Φ_Δ) in a solution.[18−20] Therefore, $^1O_2$ has been considered an important reactive species for antimicrobial effects using phenothiazine dyes.[3,6,19] However, biological environments, including the biofilms of microbes, are under hypoxic conditions.[21] Recently, we reported that these phenothiazine dyes oxidize protein through electron transfer under photoirradiation.[22] Furthermore, an analogue compound of MB, Nile blue, also induces DNA oxidation through photoinduced electron transfer.[23] Because the electron-transfer-mediated biomolecule damage does not require an oxygen molecule in the presence of other appropriate oxidative agents such as metal ions, this mechanism may play an important role in photosterilization under hypoxic conditions. In biomolecules, nicotinamide adenine dinucleotide (reduced form; NADH) is easily oxidized by the electron-transfer mechanism, and the formed radical ($NAD^\bullet$) triggers a chain reaction, leading to the acceleration of NADH decomposition and the secondary production of reactive oxygen species.[24] NADH is an important coenzyme and reductant molecule in living cells.[25,26] Thus, we examined the NADH oxidation photo-

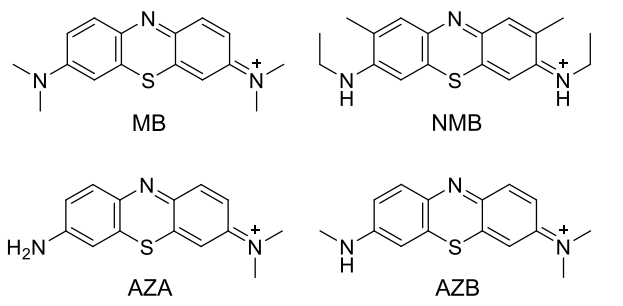

Figure 1. Structures of the phenothiazine dyes used in this study.

Received: January 26, 2021
Accepted: March 8, 2021
Published: March 17, 2021

https://doi.org/10.1021/acsomega.1c00484
ACS Omega 2021, 6, 8630−8636

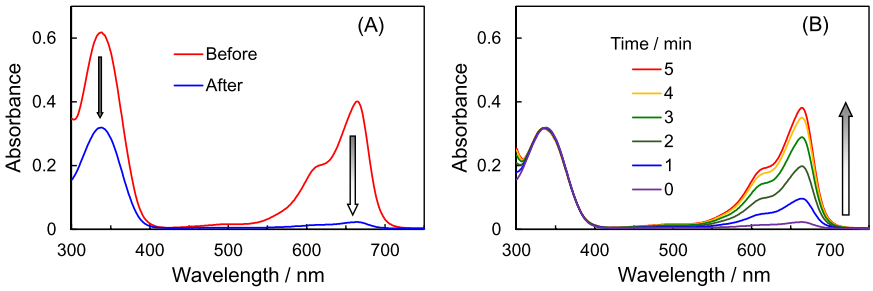

Figure 2. Absorption spectra of photoirradiated MB and NADH. The sample solution containing 5 μM MB and 100 μM NADH in a 10 mM sodium phosphate buffer (pH 7.6) was irradiated with an light-emitting diode (LED) (λ_{max} = 659 nm, 0.5 mW cm^{-2}). (A) Absorption spectra before and after photoirradiation for 20 min. (B) Time profile of the absorption spectrum in the dark after photoirradiation.

sensitized by phenothiazine dyes using MB and its derivatives (azure A (AZA), azure B (AZB), and new methylene blue (NMB); Figure 1) in this study. Specifically, the kinetic analysis was performed to investigate the mechanism of the photosensitized reaction.

RESULTS AND DISCUSSION

Photooxidation of NADH by Phenothiazine Dyes. The typical absorption of NADH at around 340 nm was decreased by photoirradiation with phenothiazine dyes (Figure 2). NADH is oxidized to NAD$^{\bullet}$ and the oxidized form (NAD^{+}) through electron transfer or reaction with reactive oxygen species, leading to the diminishing of the typical absorption. The absorption spectra of the phenothiazine dyes were also decreased during this photosensitized reaction. Figure 2 shows the case of MB. The reduction of MB produces the colorless radical form (MB$^{\bullet}$), or leucomethylene blue (LMB),[27−31] resulting in the diminishing of absorption at around 650 nm. The absorption spectra of these phenothiazine dyes recovered within several minutes under dark conditions. These results suggest that phenothiazine dyes oxidize NADH through electron extraction and that the reduced forms of phenothiazine dyes are reoxidized by oxygen to produce their corresponding cationic forms and superoxide ($O_2^{\bullet-}$).[30,31] Since the recovery of absorption spectra was observed under a dark condition, the photosensitized reaction is faster than the reoxidation process. These processes are summarized using the following equations.

$$MB^{+} + h\nu \rightarrow MB^{+}* \text{ (photoexcitation of MB)} \quad (1)$$

$$NADH + MB^{+}* \rightarrow NAD^{\bullet} + H^{+} + MB^{\bullet} \quad (2)$$

or

$$NADH + MB^{+}* \rightarrow NAD^{+} + LMB \quad (3)$$

$$MB^{\bullet} + O_2 \rightarrow MB^{+} + O_2^{\bullet-} \quad (4)$$

$$LMB + 2O_2 \rightarrow MB^{+} + 2O_2^{\bullet-} + H^{+} \quad (5)$$

where MB^{+} is the cationic form of MB and MB^{+}* is its photoexcited state.

Time Profile of the NADH Photooxidation and Scavenger Effects. The time profiles of NADH oxidation photosensitized by phenothiazine dyes are shown in Figure 3. Sodium azide (NaN_3), a physical scavenger of $^1O_2$,[32] barely inhibited the NADH photooxidation. Furthermore, potassium iodide (KI), a triplet quencher,[33] did not show an inhibitory effect on this photooxidation (Supporting Information). These results suggest that neither the triplet excited (T_1) state of

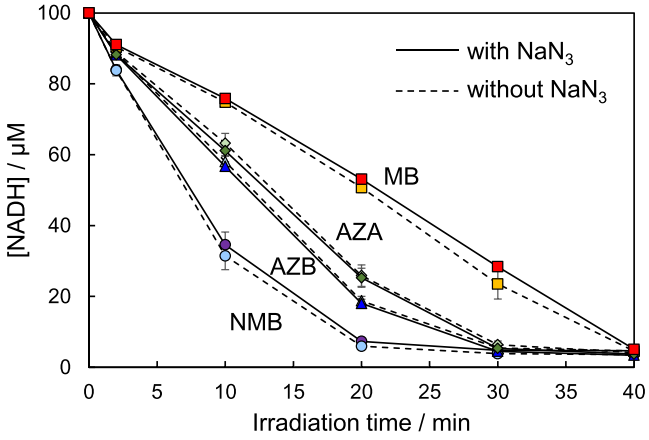

Figure 3. Time profile of the NADH decomposed by the photosensitized reaction of phenothiazine dyes. The sample solution containing 5 μM phenothiazine dye (MB, AZA, AZB, or NMB) and 100 μM NADH with or without NaN_3 in a 10 mM sodium phosphate buffer (pH 7.6) was irradiated with an LED (λ_{max}= 659 nm, 0.5 mW cm^{-2}).

these phenothiazine dyes nor $^1O_2$ are responsible for NADH oxidation. However, it is generally accepted that the T_1 states of MB and phenothiazine dyes induce oxidative electron transfer from organic molecules.[34,35] KI would serve as a reductant for the phenothiazine dye T_1 states and may lead to the formation of $O_2^{\bullet-}$ and H_2O_2.[36] The generation of these secondary reactive oxygen species could enhance NADH oxidation and might offset the inhibitory effect of KI. On the other hand, it has also been reported that the singlet excited (S_1) state of MB can oxidize organic compounds through electron transfer.[34,37] Although the possibility of a T_1 state-mediated mechanism could not be excluded, the following processes are proposed to explain the observed results. The photosensitized NADH oxidation by phenothiazine dyes can be explained by the electron extraction from NADH to the S_1 state of phenothiazine dyes (Dye^{+}*) as follows

$$NADH + Dye^{+}* \rightarrow NAD^{\bullet} + H^{+} + Dye^{\bullet} \quad (6)$$

where Dye$^{\bullet}$ is the reduced radical form of phenothiazine dyes. The Gibbs free energy (ΔG) of the electron transfer from NADH to the S_1 states of these phenothiazine dyes is negative (Table 1), supporting this mechanism from the thermodynamic point of view.

The quantum yield of NADH oxidation (Φ_{ox}) was estimated from the oxidized NADH within 10 min (Figure 3) and the photon fluence absorbed by dyes (Flu_{AP}, unit: nmol min^{-1}; Supporting Information) as follows

https://doi.org/10.1021/acsomega.1c00484
ACS Omega 2021, 6, 8630−8636

Table 1. Photochemical and Redox Parameters of Phenothiazine Dyes and the Gibbs Energy of Electron Transfer[a]

dyes	Fl_{max} (nm)	E_{S1} (eV)	E_{red} (V) vs SCE	ΔG (eV)
MB	680	1.82	−0.22[a]	−1.23
AZA	641	1.93	−0.26[b]	−1.30
AZB	668	1.86	−0.27[b]	−1.22
NMB	648	1.91	−0.29[c]	−1.25

[a]Fl_{max}: fluorescence maximum wavelength; E_{S1}: S_1 state energy of phenothiazine dyes; E_{red}: redox potential of one-electron reduction; SCE: saturated calomel electrode; a, b, and c: The values of E_{red} for a,[38] b,[39] and c[40] are according to the corresponding literatures; the fluorescence spectra of 10 μM dyes (MB, AZA, AZB, or NMB) were measured in a 10 mM sodium phosphate buffer (pH 7.6). The ΔG values were calculated using these values (Supporting Information).

$$\Phi_{ox} = \frac{[NADH_{ox}]}{Flu_{AP} \times 10\ min} \quad (7)$$

where $[NADH_{ox}]$ is the amount of oxidized NADH (unit: nmol). The calculated values are listed in Table 2. NMB

Table 2. Quantum Yields of the NADH Oxidation Processes by Photoirradiated Phenothiazine Dyes through Electron Transfer[a]

dyes	Φ_{ox}	Φ_{ET}	Φ_{rec}
MB	3.0×10^{-2}	2.7×10^{-4}	1.1×10^{2}
AZA	5.4×10^{-2}	3.4×10^{-4}	1.6×10^{2}
AZB	5.3×10^{-2}	2.5×10^{-4}	2.1×10^{2}
NMB	1.7×10^{-1}	3.4×10^{-4}	5.0×10^{2}

[a]Φ_{ox}: the total quantum yield of NADH oxidation. Φ_{ET}: the quantum yield of the electron transfer from NADH to photoexcited phenothiazine dyes. Φ_{rec}: the quantum yield of further reaction to form NAD^+. The sample solution containing 5 μM MB and 100 μM NADH with or without 10 mM NaN_3 in a 10 mM sodium phosphate buffer (pH 7.6) was irradiated with an LED (λ_{max}= 659 nm, 0.5 mW cm^{-2}). These quantum yields were calculated using eqs 7−9.

demonstrated the highest activity in the phenothiazine dyes used. This result can be explained by the fact that reduced NMB is easily reoxidized and accelerates the redox cycle (described later).

Mechanism of Photosensitized NADH Oxidation: Chain Reaction and Rate-Determining Step. The above-mentioned NADH oxidation can be explained by the electron transfer from NADH to the photoexcited state of phenothiazine dyes as shown in Figure 4. The collision between the S_1 (or T_1) states of dye molecules and NADH is the initial process of this electron-transfer reaction. In this section, the kinetics of NADH photooxidation are discussed under the

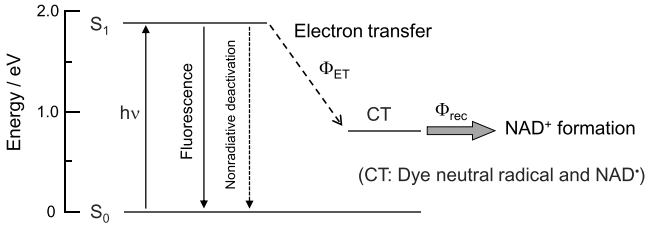

Figure 4. Relaxation processes for the photoexcited phenothiazine dyes and the photosensitized NADH oxidation.

assumption that the S_1 state of phenothiazine dyes induces oxidative electron transfer. Because the fluorescence lifetime (τ_f) (the S_1 state lifetimes) of these dyes (MB: 0.37 ns; AZA: 0.46 ns; AZB: 0.34 ns; and NMB: 0.46 ns) was barely affected by NADH, the efficiency of this electron-transfer reaction was too small to be determined under this experimental condition. Therefore, the possible quantum yield (Φ_{ET}; Table 2) of this electron transfer is expressed as follows

$$\Phi_{ET} = \frac{k_{dif}[NADH]}{k_0 + k_{dif}[NADH]} \quad (8)$$

where k_{dif} is the diffusion control reaction limit (7.4×10^9 M^{-1} s^{-1}) in this experimental condition, [NADH] is the concentration of NADH, and k_0 ($=1/\tau_f$) is the deactivation rate constant expressed using the τ_f values (same as the S_1 state lifetime). This electron transfer produces $NAD^{\bullet}$, which undergoes further reaction to produce NAD^+ (Figure 4). Using the quantum yield of this further reaction (Φ_{rec}), the Φ_{ox} can be expressed as follows

$$\Phi_{ox} = \Phi_{ET} \times \Phi_{rec} \quad (9)$$

Since the T_1 state may contribute to NADH oxidation, the estimated Φ_{rec} values are the maximum limits. Although the actual Φ_{rec} values may be smaller than these listed values (Table 2), the estimated values were much larger than 1, suggesting a chain reaction. A similar phenomenon was reported previously in the case of NADH oxidation photosensitized by porphyrin P(V) complexes.[24]

The proposed mechanism of NADH photooxidation (photoredox cycle) is shown in Figure 5. Figure 2 shows that the reduced forms of phenothiazine dyes are reoxidized to the cationic forms, resulting in the construction of a redox cycle. The reaction rate coefficients of the initial process (k_1) and the reoxidation of reduced dyes (k_2) are expressed as follows

$$\frac{d[NADH]}{dt} = -k_1[NADH][Dye] \quad (10)$$

and

$$\frac{d[Dye]}{dt} = -k_1[NADH][Dye] + k_2[Dye_{red}][O_2] \quad (11)$$

where [Dye] is the concentration of the cationic form of the phenothiazine dye, $[Dye_{red}]$ is that of the reduced form, and $[O_2]$ is the dissolved oxygen concentration (260 μM under this experimental condition).[41] The time profile of the photosensitized NADH oxidation was analyzed using a numerical calculation to estimate these rate coefficients (Table 3). The values of k_2 are much smaller than those of k_1, and a good relationship between k_2 and Φ_{ox} (correlation coefficient: 0.98) was observed (Supporting Information). These findings demonstrate that the reproduction process for cationic dyes is the rate-determining step in this photosensitized reaction. The highest photooxidative activity of NMB can be explained by the fast reoxidation of the reduced form of NMB. The calculation using density functional theory (DFT) showed that the ionization energy of reduced NMB (neutral radical form; 6.09 eV) is smaller than that of other dyes used in this study (MB: 6.10 eV; AZA: 6.20 eV; and AZB: 6.16 eV), supporting the fast reoxidation of the reduced NMB.

Formation of Superoxide during the Photosensitized Reaction. The above-mentioned mechanism (Figure 5)

https://doi.org/10.1021/acsomega.1c00484
ACS Omega 2021, 6, 8630−8636

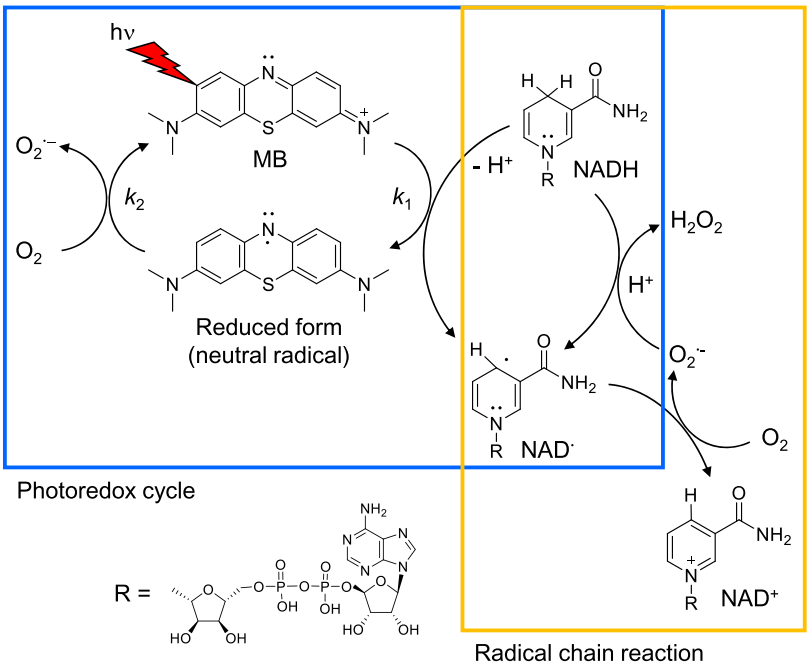

Figure 5. Proposed mechanism of NADH decomposition by phenothiazine dyes through photoredox cycle and chain reaction.

Table 3. Kinetic Parameters of NADH Oxidation Photosensitized by Phenothiazine Dyes[a]

dyes	k_1 (M^{-1} s^{-1})	k_2 (M^{-1} s^{-1})	k_2' (M^{-1} s^{-1})
MB	25.0	0.28	2.42
AZA	21.7	0.70	10.0
AZB	33.3	1.25	11.7
NMB	17.5	4.50	66.7

[a]The sample solution contained 10 μM phenothiazine dyes and 100 μM NADH with or without 0.1 μM Cu^{2+} in a 10 mM sodium phosphate buffer (pH 7.6). The irradiation condition was the same as that in Table 2. The k_2' is the rate coefficient of reoxidation in the presence of 0.1 μM Cu^{2+}. To analyze the NADH photooxidation by phenothiazine dyes with Cu^{2+}, the same values were used for the k_1 in this table.

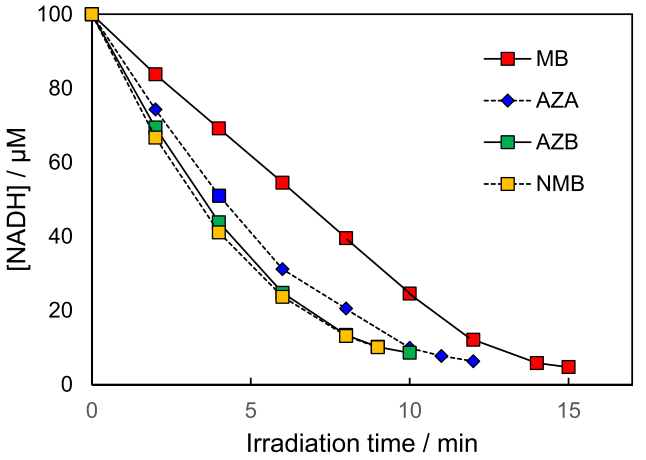

Figure 6. Time profile of the NADH decomposed by the photosensitized reaction of phenothiazine dyes with Cu^{2+}. The sample solution containing 5 μM phenothiazine dye (MB, AZA, AZB, or NMB), 100 μM NADH, and 0.1 μM Cu^{2+} in a 10 mM sodium phosphate buffer (pH 7.6) was irradiated with an LED (λ_{max} = 659 nm, 0.5 mW cm^{-2}).

predicts the formation of $O_2^{\bullet-}$ in the presence of an oxygen molecule.[24,42] The formation of $O_2^{\bullet-}$ was evaluated using the cytochrome *c* reduction method (Supporting Information). The order of $O_2^{\bullet-}$ formation rates in this experimental condition was as follows: MB (9.6×10^{-2} μM s^{-1}) > AZB (3.4×10^{-2} μM s^{-1}) > NMB (3.0×10^{-2} μM s^{-1}) > AZA (2.7×10^{-2} μM s^{-1}). The kinetics of $O_2^{\bullet-}$ formation are complex because the possible other processes of $O_2^{\bullet-}$ formation are the reoxidation of reduced dyes and the oxidation of NAD$^{\bullet}$, and $O_2^{\bullet-}$ is consumed to produce hydrogen peroxide (H_2O_2).[29,35,36] Therefore, this order of $O_2^{\bullet-}$ formation rates could not be explained well; however, these results support the proposed mechanism in Figure 5 and suggest the secondary formation of reactive oxygen species, $O_2^{\bullet-}$ and H_2O_2, during these photosensitized reactions. A similar result has been reported previously.[24]

Effect of a Copper Ion on the Photosensitized Reaction. The addition of a copper ion (Cu^{2+}) markedly enhanced the photosensitized NADH oxidation by phenothiazine dyes (Figure 6). Copper is an important endogenous metal.[43,44] It has been reported that Cu^{2+} can reoxidize the reduced form of MB to the initial cationic form.[29] In the presence of 5 μM Cu^{2+} (equimolar quantity of dyes in this experimental condition), the reduced phenothiazine dyes were immediately reoxidized to their cationic forms (data not shown), suggesting that this reaction is very fast. Analysis of the time profile using a method similar to that in Figure 3 indicated the increase of k_2 values by Cu^{2+} and enhancement of the reoxidation process of reduced dyes (Table 3). The role of Cu^{2+} could be speculated as shown in Figure 7, similar to the literature.[29] The copper ion catalyzes the reoxidation of the reduced dyes. Because the reoxidation of the reduced dyes by Cu^{2+} is very fast, the reproduction of Cu^{2+} from Cu^{+} through the oxidation by oxygen is the rate-determining step. These results suggest that the endogenous metal ions play an important role in photosensitized NADH oxidation. In the

https://doi.org/10.1021/acsomega.1c00484
ACS Omega 2021, 6, 8630−8636

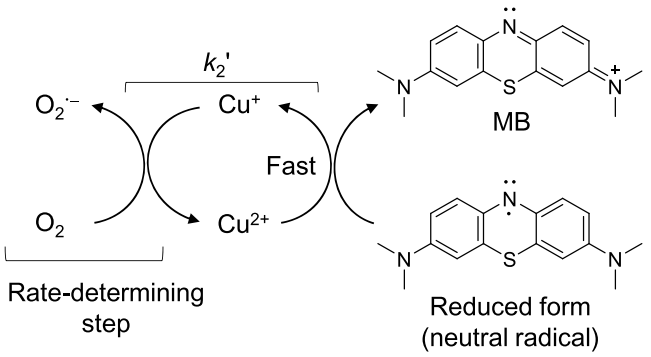

Figure 7. Scheme of the accelerated reoxidation process by Cu^{2+}.

case of NMB, the rate coefficient of reoxidation became larger than that of the electron-transfer rate coefficient.

CONCLUSIONS

Phenothiazine dyes photosensitized NADH oxidation through electron transfer. The S_1 (or T_1) state of phenothiazine dyes extracts electrons from NADH through diffusion and collision. The reduced forms of these phenothiazine dyes undergo reoxidation to the original cationic forms, leading to the construction of a photoredox cycle. This reoxidation process is the rate-determining step in the photosensitized NADH oxidation. The $NAD^{\bullet}$ formed through this electron transfer can trigger the chain reaction of the NADH oxidation (Figure 5). Secondary reactive oxygen species, $O_2^{\bullet-}$ and H_2O_2, can be produced during this chain reaction in the presence of oxygen molecules. Copper ions enhance the photoredox cycle through reoxidation of the reduced forms of phenothiazine dyes. Endogenous metal ions may play an important role in photosensitized NADH oxidation in biological environments. In this study, NMB demonstrated the highest photooxidative activity due to the fast reoxidation process of the reduced form of NMB. Electron-transfer-mediated oxidation and the role of endogenous metal ions may be important in the photosterilization mechanism.

EXPERIMENTAL SECTION

Materials. MB and KI were purchased from Kanto Chemical Co., Inc. (Tokyo, Japan). AZA, AZB, and superoxide dismutase (SOD) were from Sigma-Aldrich Co. LLC. (St. Louis, MO). Copper chloride, cytochrome *c*, and NaN_3 were from FUJIFILM Wako Pure Chemical Co. (Osaka, Japan). NMB was from Tokyo Chemical Industry Co., Ltd. (Tokyo, Japan). NADH and sodium phosphate buffer (0.1 M, pH 7.6) were from Nacalai Tesque, Inc. (Kyoto, Japan). These reagents were used as received.

Measurements. The absorption spectra of phenothiazine dyes and NADH were measured with a UV−vis spectrophotometer UV-1650PC (Shimadzu, Kyoto, Japan). The fluorescence spectra of the samples were measured with an F-4500 fluorescence spectrophotometer (Hitachi, Tokyo, Japan). The τ_f of phenothiazine dyes was measured using a time-correlated single-photon counting method with the TemPro Fluorescence Lifetime System (HORIBA, Kyoto, Japan). Laser excitation at 637 nm was achieved using a diode laser (NanoLED-635L, HORIBA) at a repetition rate of 1.0 MHz. The experimental error of this measurement is within 0.01 ns.

Determination of Photosensitized NADH Oxidation. The sample solution containing phenothiazine dyes and NADH in a 10 mM sodium phosphate buffer (pH 7.6) was irradiated with a light-emitting diode (LED) (λ_{max}= 659 nm, 0.5 mW cm^{-2}, CCS Inc., Kyoto, Japan). The intensity of the LED light source (unit: mW cm^{-2}) was measured with an 8230E optical power meter (ADC Corporation, Tokyo, Japan). The Flu_{AP} was estimated from the observed intensity of the LED and the absorption spectrum of the dyes (Supporting Information). The photosensitized NADH oxidation by phenothiazine dyes was evaluated by measuring the absorbance of NADH at 340 nm as previously reported.[24] The [$NADH_{ox}$] was estimated from this absorbance change (Supporting Information).

Calculations. The optimized structure and energy of reduced phenothiazine dyes (neutral radical forms) were calculated using the DFT method at the ωB97X-D/6-31G* level utilizing the Spartan 18′ (Wavefunction Inc., CA).

Measurement of Superoxide Formation. The quantity of superoxide ($O_2^{\bullet-}$) formation during the photosensitized reaction was determined using the cytochrome *c* reduction method.[45] The sample solution containing 50 μM ferricytochrome *c*, 100 μM NADH, and 5 μM phenothiazine dyes with or without 150 U mL^{-1} SOD in 1.2 mL of 10 mM sodium phosphate buffer (pH 7.6) was irradiated. The absorption at 550 nm (molar absorption coefficient: 21 100 M^{-1} cm^{-1})[45] was measured with the UV−vis spectrophotometer UV-1650PC (Shimadzu), and the quantity of reduced cytochrome *c* was then calculated to determine the $O_2^{\bullet-}$ formation.

ASSOCIATED CONTENT

Supporting Information

The Supporting Information is available free of charge at https://pubs.acs.org/doi/10.1021/acsomega.1c00484.

Calculation of the photon fluence absorbed by dyes; calculation of the oxidized NADH concentration; effect of potassium iodide; fluorescence spectra of phenothiazine dyes; ΔG values of electron transfer; relationship between the rate coefficient and quantum yield; and estimation of superoxide formation (PDF)

AUTHOR INFORMATION

Corresponding Author

Kazutaka Hirakawa − *Applied Chemistry and Biochemical Engineering Course, Department of Engineering, Graduate School of Integrated Science and Technology and Department of Optoelectronics and Nanostructure Science, Graduate School of Science and Technology, Shizuoka University, Hamamatsu, Shizuoka 432-8561, Japan;* orcid.org/0000-0002-3694-8165; Phone: +81-53-478-1287; Email: hirakawa.kazutaka@shizuoka.ac.jp

Author

Mizuho Mori − *Applied Chemistry and Biochemical Engineering Course, Department of Engineering, Graduate School of Integrated Science and Technology, Shizuoka University, Hamamatsu, Shizuoka 432-8561, Japan*

Complete contact information is available at: https://pubs.acs.org/10.1021/acsomega.1c00484

Notes

The authors declare no competing financial interest.

https://doi.org/10.1021/acsomega.1c00484
ACS Omega 2021, 6, 8630−8636

■ ACKNOWLEDGMENTS

This work was supported in part by Grant-in-Aid for Scientific Research (B) from the Japanese Society for the Promotion of Science (JSPS KAKENHI 17H03086).

■ REFERENCES

(1) Tardivo, J. P.; Del Giglio, A.; de Oliveira, C. S.; Gabrielli, D. S.; Junqueira, H. C.; Tada, D. B.; Severino, D.; de Fátima, T. R.; Baptista, M. S. Methylene Blue in Photodynamic Therapy: From Basic Mechanisms to Clinical Applications. *Photodiagn. Photodyn. Ther.* **2005**, *2*, 175−191.
(2) Spagnul, C.; Turner, L. C.; Boyle, R. W. Immobilized Photosensitizers for Antimicrobial Applications. *J. Photochem. Photobiol., B* **2015**, *150*, 11−30.
(3) Wainwright, M.; O'Kane, C.; Rawthore, S. Phenothiazinium Photosensitisers XI. Improved Toluidine Blue Photoantimicrobials. *J. Photochem. Photobiol., B* **2016**, *160*, 68−71.
(4) Wainwright, M.; McLean, A. Rational Design of Phenothiazinium Derivatives and Photoantimicrobial Drug Discovery. *Dyes Pigm.* **2017**, *136*, 590−600.
(5) de Freitas, M. T. M.; Soares, T. T.; Aragão, M. G. B.; Lima, R. A.; Duarte, S.; Zanin, I. C. J. Effect of Photodynamic Antimicrobial Chemotherapy on Mono- and Multi-Species Cariogenic Biofilms: a Literature Review. *Photomed. Laser Surg.* **2017**, *35*, 239−245.
(6) Tim, M. Strategies to Optimize Photosensitizers for Photodynamic Inactivation of Bacteria. *J. Photochem. Photobiol., B* **2015**, *150*, 2−10.
(7) Ma, W.; Liu, C.; Li, J.; Hao, M.; Ji, Y.; Zeng, X. The Effects of Aloe Emodin-Mediated Antimicrobial Photodynamic Therapy on Drug-Sensitive and Resistant Candida Albicans. *Photochem. Photobiol. Sci.* **2020**, *19*, 485−494.
(8) Singhal, G. S.; Rabinowitch, E. Changes in the Absorption Spectrum of Methylene Blue with pH. *J. Phys. Chem. A* **1967**, *71*, 3347−3349.
(9) Anderson, R. R.; Parrish, J. A. The Optics of Human Skin. *J. Invest. Dermatol.* **1981**, *77*, 13−19.
(10) Mallidi, S.; Anbil, S.; Bulin, A.-L.; Obaid, G.; Ichikawa, M.; Hasa, T. Beyond the Barriers of Light Penetration: Strategies, Perspectives and Possibilities for Photodynamic Therapy. *Theranostics* **2016**, *6*, 2458−2487.
(11) Joseph, B.; Janam, P.; Narayanan, S.; Anil, S. Is Antimicrobial Photodynamic Therapy Effective As an Adjunct to Scaling and Root Planing in Patients with Chronic Periodontitis? A Systematic Review. *Biomolecules* **2017**, *7*, No. 79.
(12) Cao, R.; Li, Q.; Wu, Q.; Yao, M.; Chen, Y.; Zhou, H. Effect of Non-Surgical Periodontal Therapy on Glycemic Control of Type 2 Diabetes Mellitus: A Systematic Review and Bayesian Network Meta-Analysis. *BMC Oral Health* **2019**, *19*, No. 176.
(13) de Oliveira, A. B.; Ferrisse, T. M.; Marques, R. S.; de Annunzio, S. R.; Brighenti, F. L.; Fontana, C. R. Effect of Photodynamic Therapy on Microorganisms Responsible for Dental Caries: A Systematic Review and Meta-Analysis. *Int. J. Mol. Sci.* **2019**, *20*, No. 3585.
(14) Méndez, D. A. C.; Gutierrez, E.; Dionísio, E. J.; Oliveira, T. M.; Buzalaf, M. A. R.; Rios, D.; Machado, M. A. A. M.; Cruvinel, T. Effect of Methylene Blue-Mediated Antimicrobial Photodynamic Therapy on Dentin Caries Microcosms. *Lasers Med. Sci.* **2018**, *33*, 479−487.
(15) Rosa, L. P.; da Silva, F. C.; Nader, S. A.; Meira, G. A.; Viana, M. S. Effectiveness of Antimicrobial Photodynamic Therapy Using a 660 nm Laser and Methylene Blue Dye for Inactivating Staphylococcus Aureus Biofilms in Compact and Cancellous Bones: an In Vitro Study. *Photodiagn. Photodyn. Ther.* **2015**, *12*, 276−281.
(16) Floyd, R. A.; Schneider, J. E., Jr.; Dittmer, D. P. Methylene Blue Photoinactivation of RNA Viruses. *Antiviral Res.* **2004**, *61*, 141−151.
(17) Huang, Q.; Fu, W.-L.; Chen, B.; Huang, J.-F.; Zhang, X.; Xue, Q. Inactivation of Dengue Virus by Methylene Blue/Narrow Bandwidth Light System. *J. Photochem. Photobiol., B* **2004**, *77*, 39−43.
(18) Usui, Y.; Kamogawa, K. A Standard System to Determine the Quantum Yield of Singlet Oxygen Formation in Aqueous Solution. *Photochem. Photobiol.* **1974**, *19*, 245−247.
(19) DeRosa, M. C.; Crutchley, R. J. Photosensitized Singlet Oxygen and Its Applications. *Coord. Chem. Rev.* **2002**, *233/234*, 351−371.
(20) Hirakawa, K. Fluorometry of Singlet Oxygen Generated via a Photosensitized Reaction Using Folic Acid and Methotrexate. *Anal. Bioanal. Chem.* **2009**, *393*, 999−1005.
(21) Jørgensen, E.; Bay, L.; Bjarnsholt, T.; Bundgaard, L.; Sørensen, M. A.; Jacobsen, S. The Occurrence of Biofilm in an Equine Experimental Wound Model of Healing by Secondary Intention. *Vet. Microbiol.* **2017**, *204*, 90−95.
(22) Hirakawa, K.; Ishikawa, T. Phenothiazine Dyes Photosensitize Protein Damage through Electron Transfer and Singlet Oxygen Generation. *Dyes Pigm.* **2017**, *142*, 183−188.
(23) Hirakawa, K.; Ota, K.; Hirayama, J.; Oikawa, S.; Kawanishi, S. Nile Blue Can Photosensitize DNA Damage through Electron Transfer. *Chem. Res. Toxicol.* **2014**, *27*, 649−655.
(24) Hirakawa, K.; Murata, A. Photosensitized Oxidation of Nicotinamide Adenine Dinucleotide by Diethoxyphosphorus(V)-tetraphenylporphyrin and Its Fluorinated Derivative: Possibility of Chain Reaction. *Spectrochim. Acta, Part A* **2018**, *188*, 640−646.
(25) Begley, T. P.; Kinsland, C.; Mehl, R. A.; Osterman, A.; Dorrestein, P. The Biosynthesis of Nicotinamide Adenine Dinucleotides in Bacteria. *Vitam. Horm.* **2001**, *61*, 103−119.
(26) Anderson, K. A.; Madsen, A. S.; Olsen, C. A.; Hirschey, M. D. Metabolic Control by Sirtuins and Other Enzymes that Sense NAD^+, NADH, or Their Ratio. *Biochim. Biophys. Acta, Bioenerg.* **2017**, *1858*, 991−998.
(27) de Araujo Nicolai, S. H.; Rodrigues, P. R. P.; Agostinho, S. M. L.; Rubim, J. C. Electrochemical and Spectroelectrochemical (SERS) Studies of the Reduction of Methylene Blue on a Silver Electrode. *J. Electroanal. Chem.* **2002**, *527*, 103−111.
(28) Caram, J. A.; Suárez, J. F. M.; Gennaro, A. M.; Mirífico, M. V. Electrochemical Behavior of Methylene Blue in Non-Aqueous Solvents. *Electrochim. Acta* **2015**, *164*, 353−363.
(29) Hiraku, Y.; Goto, H.; Kohno, M.; Kawanishi, S.; Murata, M. Metal-Mediated Oxidative DNA Damage Induced by Methylene Blue. *Biochim. Biophys. Acta, Gen. Subj.* **2014**, *1840*, 2776−2782.
(30) Sevcik, P.; Dunford, H. B. Kinetics of the Oxidation of NADH by Methylene Blue in a Closed System. *J. Phys. Chem. B* **1991**, *95*, 2411−2415.
(31) Carson, J. J. L.; Walleczek, J. Response of the Peroxidase-Oxidase Oscillator to Light Is Controlled by MB^+−NADH Photochemistry. *J. Phys. Chem. B* **2003**, *107*, 8637−8642.
(32) Li, M. Y.; Cline, C. S.; Koker, E. B.; Carmichael, H. H.; Chignell, C. F.; Bilski, P. Quenching of Singlet Molecular Oxygen ($^1O_2$) by Azide Anion in Solvent Mixtures. *Photochem. Photobiol.* **2001**, *74*, 760−764.
(33) Lessard, G.; Durocher, G. Singlet and Triplet Quenching of Indole by Heavy Atom Containing Molecules in a Low Temperature Glassy Matrix. Evidence for Complexation in the Triplet State. *J. Phys. Chem. C* **1978**, *82*, 2812−2819.
(34) Bertolotti, S. G.; Previtali, C. M. The Excited States Quenching of Phenothiazine Dyes by p-Benzoquinones in Polar Solvents. *Dyes Pigm.* **1999**, *41*, 55−61.
(35) Görner, H. Oxygen Uptake Induced by Electron Transfer from Donors to the Triplet State of Methylene Blue and Xanthene Dyes in Air-saturated Aqueous Solution. *Photochem. Photobiol. Sci.* **2008**, *7*, 371−376.
(36) Kawai, K.; Kodera, H.; Majima, T. Photocatalytic Formation of I-I Bonds Using DNA Which Enables Detection of Single Nucleotide Polymorphisms. *J. Am. Chem. Soc.* **2010**, *132*, 14216−14220.
(37) Manring, L. E.; Eriksen, J.; Foote, C. S. Electron-transfer Photooxygenation. 4. Photooxygenation of trans-Stilbene Sensitized by Methylene Blue. *J. Am. Chem. Soc.* **1980**, *102*, 4275−4277.
(38) Kelley, S. O.; Barton, J. K.; Jackson, N. M.; Hill, M. G. Electrochemistry of Methylene Blue Bound to a DNA-Modified Electrode. *Bioconjugate Chem.* **1997**, 31−37.

https://doi.org/10.1021/acsomega.1c00484
ACS Omega 2021, 6, 8630−8636

(39) Brunetti, B.; Ugo, P.; Moretto, L. M.; Martin, C. R. Electrochemistry of Phenothiazine and Methylviologen Biosensor Electron-Transfer Mediators at Nanoelectrode Ensembles. *J. Electroanal. Chem.* **2000**, *491*, 166−174.
(40) Paul, P.; Mati, S. S.; Bhattacharya, S. C.; Kumar, G. S. Spectroscopic, Calorimetric, Cyclic Voltammetric and Molecular Modeling Studies of New Methylene Blue-Polyadenylic Acid Interaction and Comparison to Thionine and Toluidine Blue O: Understanding Self-Structure Formation by Planar Dyes. *Dyes Pigm.* **2017**, *136*, 205−218.
(41) Hirakawa, K.; Umemoto, H.; Kikuchi, R.; Yamaguchi, H.; Nishimura, Y.; Arai, T.; Okazaki, S.; Segawa, H. Determination of Singlet Oxygen and Electron Transfer Mediated Mechanisms of Photosensitized Protein Damage by Phosphorus(V)porphyrins. *Chem. Res. Toxicol.* **2015**, *28*, 262−267.
(42) Goldstein, S.; Czapski, G. Reactivity of Peroxynitrite versus Simultaneous Generation of •NO and O_2•$^-$ toward NADH. *Chem. Res. Toxicol.* **2000**, *13*, 736−741.
(43) Burkitt, M. J. Copper−DNA Adducts. *Methods Enzymol.* **1994**, *234*, 66−79.
(44) Koh, E.-I.; Henderson, J. P. Microbial Copper-Binding Siderophores at the Host-Pathogen Interface. *J. Biol. Chem.* **2015**, *290*, 18967−18974.
(45) Murata, M.; Kawanishi, S. Oxidative DNA Damage by Vitamin A and Its Derivative via Superoxide Generation. *J. Biol. Chem.* **2000**, *275*, 2003−2008.

https://doi.org/10.1021/acsomega.1c00484
ACS Omega 2021, 6, 8630−8636